



Investigation of the intestinal trans-epithelial transport and antioxidant activity of two hempseed peptides WVSPLAGRT (H2) and IGFLIIWV (H3)

Carlotta Bollati^a, Ivan Cruz-Chamorro^{a,b}, Gilda Aiello^c, Jianqiang Li^a, Martina Bartolomei^a, Guillermo Santos-Sánchez^{a,b}, Giulia Ranaldi^d, Simonetta Ferruzza^d, Yula Sambuy^d, Anna Arnoldi^a, Carmen Lammi^{a,*}

^a Department of Pharmaceutical Sciences, University of Milan, 20133 Milan, Italy

^b Departamento de Bioquímica Médica y Biología Molecular e Inmunología, Universidad de Sevilla, 41009 Seville, Spain

^c Department of Human Science and Quality of Life Promotion, Telematic University San Raffaele, 00166 Rome, Italy

^d CREA, Food and Nutrition Research Centre, Via Ardeatina, 546, 00178 Roma RM, Italy

ARTICLE INFO

Keywords:

Antioxidant peptides
Bioactive peptides
Hempseed peptides
Nrf-2
ROS

ABSTRACT

A preceding paper has shown that a hempseed peptic hydrolysate displays a cholesterol-lowering activity with a statin-like mechanism of action in HepG2 cells and a potential hypoglycemic activity by the inhibition of dipeptidyl peptidase-IV in Caco-2 cells. In the framework of a research aimed at fostering the multifunctional behavior of hempseed peptides, we present here the identification and evaluation of some antioxidant peptides from the same hydrolysate. After evaluation of its diphenyl-2-picrylhydrazyl (DPPH) radical scavenging activity, a trans-epithelial transport experiment was performed using differentiated Caco-2 cells that permitted the identification of five transported peptides that were synthesized and evaluated by measuring the oxygen radical absorbance capacity (ORAC), the ferric reducing antioxidant power (FRAP), and the 2,2-azino-bis-(3-ethylbenzothiazoline-6-sulfonic) acid (ABTS), and diphenyl-2-picrylhydrazyl radical DPPH assays. The most active peptides, i.e. WVSPLAGRT (H2) and IGFLIIWV (H3), were then tested in cell assays. Both peptides were able to reduce the H₂O₂-induced reactive oxygen species (ROS), lipid peroxidation, and nitric oxide (NO) production levels in HepG2 cells, via the modulation of Nrf-2 and iNOS pathways, respectively.

1. Introduction

The seed of industrial hemp, i.e. the non-drug cultivars of *Cannabis sativa*, stands out for its high protein (~25%) content (Callaway, 2004). The superior amino acid profile and high digestibility of hempseed proteins suggests their potential efficacy as a source of health-promoting peptides. In fact, different Authors have investigated the biological activity of peptides produced by hydrolyzing hempseed protein with different enzymes.

Due to the heterogeneous composition of the protein hydrolysates, it is likely that these materials may provide more the one biological activity (Lammi, Aiello, Boschin, & Arnoldi, 2019). This multifunctional behavior has been clearly highlighted for hempseed hydrolysates (Farinon, Molinari, Costantini, & Merendino, 2020). In fact, hempseed peptides, obtained hydrolyzing the proteins with a combination of pepsin and pancreatin, possess both antioxidant and hypotensive

activity either *in vitro* or *in vivo* (Girgih et al., 2014). The antioxidant and antihypertensive effects may be due to the presence of high levels of negatively charged amino acids for electron donation to reactive oxygen species and arginine for the production of nitric oxide (NO), a vasodilating agent, respectively. The hypotensive activity may depend also on the inhibition of angiotensin-converting enzyme (ACE) and renin (Girgih, He, & Aluko, 2014; Girgih et al., 2014). Other Authors have demonstrated, instead, that specific hempseed hydrolysate fractions are either antioxidant or neuroprotective (Rodríguez-Martin et al., 2019). Furthermore, hempseed protein hydrolysates obtained by different hydrolysis methods have *in vitro* neuroprotective activity (Malomo & Aluko, 2016) and *in vitro* and *in vivo* hypotensive activity (Malomo, Onuh, Girgih, & Aluko, 2015).

In addition, a recent investigation by our group has shown that a hydrolysate obtained digesting a total protein extract from hempseed with pepsin (HP) displays cholesterol-lowering activity through the

* Corresponding author at: Department of Pharmaceutical Sciences, University of Milan, via Mangiagalli 25, 20133 Milan, Italy.

E-mail address: carmen.lammi@unimi.it (C. Lammi).

<https://doi.org/10.1016/j.foodres.2021.110720>

Received 17 June 2021; Received in revised form 26 August 2021; Accepted 20 September 2021

Available online 22 September 2021

0963-9969/© 2021 Elsevier Ltd. All rights reserved.

inhibition of 3-hydroxy-3-methyl-glutaryl-coenzyme A reductase (HMGCoAR) (C Lammi, Bollati, Gelain, Arnoldi, & Pugliese, 2019; Zanoni, Aiello, Arnoldi, & Lammi, 2017). This inhibition leads to a positive low-density lipoprotein (LDL) receptor (LDLR) pathway modulation in human hepatic HepG2 cells (Zanoni et al., 2017). Finally, HP is also able to inhibit dipeptidyl peptidase-IV (DPP-IV), either *in vitro* on the human recombinant enzyme or in human intestinal Caco-2 cells, suggesting a potential anti-diabetic effect (Lammi et al., 2019).

Considering that there is currently a big interest for antioxidant peptides from dietary sources, the present study was aimed at fostering the multifunctional health promoting activities of hempseed peptides focusing the interest on the identification and characterization of bioavailable antioxidant peptides. More in details, the first objective of the work was the assessment of the antioxidant activity of the HP hydrolysate using the 1,1-diphenyl-2-picrylhydrazyl radical (DPPH) assay.

As the bioavailability is always a crucial feature, the second objective of the study was the identification of bioavailable peptides in the HP hydrolysate. In fact, we have developed a strategy for identifying bioavailable and active peptides based on the use of differentiated Caco-2 cell: in practice, the differentiated Caco-2 monolayer is used as a “natural sieve of bioavailable species”. This permits to concentrate further research exclusively on absorbable peptides (Lammi et al., 2016).

The third objective of the work was the evaluation of the activity of absorbed peptides. To achieve this goal, the transported ones were synthesized and their direct antioxidant activity was tested using the most important antioxidant test [DPPH, oxygen radical absorbance capacity (ORAC), ferric reducing antioxidant power (FRAP), and 2,2-azino-bis-(3-ethylbenzothiazoline-6-sulfonic) acid (ABTS)]. The two most active peptides were further investigated in human hepatic HepG2 cells after the induction of oxidative stress using H₂O₂ for assessing their ability to reduce the level of reactive oxygen species (ROS), lipid peroxidation, and NO production. Finally, the effects of both peptides on the activation of nuclear factor erythroid 2-related factor 2 (Nrf-2) and inducible nitric oxide synthase (iNOS) pathway modulations were investigated in the same cells by performing western blotting experiments.

2. Material & methods

2.1. Chemicals

All chemicals and reagents were of analytical grade. Dulbecco's modified Eagle's medium (DMEM), stable L-glutamine, fetal bovine serum (FBS), phosphate buffered saline (PBS), penicillin/streptomycin, chemiluminescent reagent, and 96-well plates were purchased from Euroclone (Milan, Italy). ROS and lipid peroxidation (MDA) assay kits, Griess reagent, bovine serum albumin (BSA), RIPA buffer, the anti-Nrf2 and anti-β-actin antibodies were from Sigma-Aldrich (St. Louis, MO, USA). The iNOS primary antibody came from Cell Signaling Technology (Danvers, MA, USA). The HepG2 cell line was bought from ATCC (HB-8065, ATCC from LGC Standards, Milan, Italy) and Caco-2 cells were obtained from INSERM (Paris, France). The synthetic peptides H1, H2, H3, H4, and H5 were synthesized by the company GeneScript (Piscataway, NJ, USA) at >95% purity.

2.2. Preparation and analysis of the peptic hydrolysate from hempseed protein (HP)

Hempseeds (*C. sativa* cultivar Futura) were provided by the Institute of Agricultural Biology and Biotechnology, CNR (Milan, Italy). The isolation of hempseed proteins, their hydrolysis and peptidomic analysis was previously carried out applying methods already published (Zanoni et al., 2017). Briefly, 2 g of defatted hempseed flour were homogenized with 15 mL of 100 mM Tris-HCl/0.5 M NaCl buffer, pH 8.0. The extraction was performed in batch at 4 °C overnight under magnetic

stirring. The solid residue was eliminated by centrifugation at 6800g for 30 min at 4 °C, and the supernatant was dialyzed against 100 mM Tris-HCl buffer, pH 8.0 for 36 h at 4 °C. The protein content was assessed according to the method of Bradford, using BSA as standard. The hydrolysis was performed on the total protein extract, changing the pH from 8 to 2 by adding 1 M HCl. The pepsin solution (4 mg/mL in NaCl 30 mM) was added in a ratio 1:50 enzyme/hempseed protein (w/w). The mixture was incubated for 16 h at 37 °C and then the enzyme inactivated changing the pH to 7.8 by adding 1 M NaOH. The sample was fractionated by ultrafiltration, using membranes with a 3-kDa molecular weight cutoff (MWCO; Millipore, U.S.A.). This permeate solution was used for investigating the biological activity. For determining its composition, it was acidified with 0.1% of formic acid, and then analyzed on a SL IT mass spectrometer interfaced with a HPLC Chip Cube source (Agilent Technologies, Palo Alto, CA, U.S.A.). Separation was carried out in gradient mode at a 300 nL/min flow. The LC solvent A was 95% water, 5% ACN, and 0.1% formic acid, and solvent B was 5% water, 95% ACN, and 0.1% formic acid.

The nano pump gradient program was as follows: 5% solvent B (0 min), 80% solvent B (0–40 min), 95% solvent B (40–45 min), and back to 5% in 5 min. The drying gas temperature was 300 °C, and flow rate was 3 L/min (nitrogen). Data acquisition occurred in positive ionization mode. Capillary voltage was –1950 V, with an end plate offset of –500 V. Full scan mass spectra were acquired in the mass range from *m/z* 300 to 2000 Da. LC-MS/MS analysis was performed in data dependent acquisition AutoMS(n) mode. The MS/MS data were analyzed by Spectrum Mill Proteomics Workbench (Rev B.04.00, Agilent Technologies, Palo Alto, CA, U.S.A.) consulting NCBI_Cannabis sativa (531 sequences) protein sequences database. Two missed cleavages were allowed to pepsin; peptide mass tolerance was set to 1.2 Da and fragment mass tolerance to 0.9 Da. The threshold used for peptide identification score was ≥6; the scored peak intensity SPI% was ≥70%; and the autovalidation strategy either in peptide mode and in protein polishing was performed using an FDR cutoff of ≤1.2%.

2.3. Intestinal trans-epithelial transport of hempseed hydrolysate assessment

2.3.1. Caco-2 cell culture Caco-2 differentiation conditions

Human intestinal Caco-2 cells were cultured in DMEM high glucose with stable L-glutamine, supplemented with 10% FBS, 100 U/mL penicillin, 100 µg/mL streptomycin (complete growth medium) with incubation at 37 °C under 5% CO₂ atmosphere, according to a published protocol (Lammi et al., 2016). For differentiation, Caco-2 cells were seeded on polycarbonate filters, 12 mm diameter, 0.4 µm pore diameter (Transwell, Corning Inc., Lowell, MA, US) at a 3.5 × 10⁵ cells/cm² density in complete medium supplemented with 10% FBS in both apical (AP) and basolateral (BL) compartments for 2 d to allow the formation of a confluent cell monolayer. Starting from day three after seeding, cells were transferred to FBS-free medium in both compartments, supplemented with ITS (final concentration 10 mg/L insulin (I), 5.5 mg/L transferrin (T), 6.7 µg/L sodium selenite (S) (GIBCO-Invitrogen, San Giuliano Milanese, Italy) only in the BL compartment, and allowed to differentiate for 18–21 days with regular medium changes three times weekly (Ferruzza, Rossi, Sambuy, & Scarino, 2013).

2.3.2. Evaluation of the cell monolayer integrity

The transepithelial electrical resistance (TEER) of differentiated Caco-2 cells was measured at 37 °C using the voltmeter apparatus Millicell (Millipore Co., Billerica, MA, USA), immediately before and at the end of the transport experiments. In addition, at the end of transport experiments, cells were incubated with 1 mM phenol-red in PBS containing Ca⁺⁺ (0.9 mM) and Mg⁺⁺ (0.5 mM) for 1 h at 37 °C, to monitor the paracellular permeability of the cell monolayer. The BL solutions were then collected and NaOH (70 µL, 0.1 N) was added before reading the absorbance at 560 nm by a microplate reader Synergy

H1 from Biotek (Winooski, VT, USA). Phenol-red passage was quantified using a standard phenol-red curve. Only filters showing TEER values and phenol red passages similar to untreated control cells were considered for peptide transport analysis.

2.3.3. Trans-epithelial transport experiments

Prior to experiments, the cell monolayer integrity and differentiation were checked by TEER measurement as described in detail above. Peptide trans-epithelial passage was assayed in differentiated Caco-2 cells in transport buffer solution (137 mM NaCl, 5.36 mM KCl, 1.26 mM CaCl₂, and 1.1 mM MgCl₂, 5.5 mM glucose) according to previously described conditions. In order to reproduce the pH conditions existing *in vivo* in the small intestinal mucosa, the AP solutions were maintained at pH 6.0 (buffered with 10 mM morpholinoethane sulfonic acid), and the BL solutions were maintained at pH 7.4 (buffered with 10 mM N-2-hydroxyethylpiperazine-N-4-butananesulfonic acid). Prior to transport experiments, cells were washed twice with 500 μ L PBS containing Ca⁺⁺ and Mg⁺⁺. Peptide transportation by mature Caco-2 cells was assayed by loading the AP compartment with 1.0 mg/mL of HP hydrolysate in the AP transport solution (500 μ L) and the BL compartment with the BL transport solution (700 μ L). The plates were incubated at 37 °C and the BL solutions were collected at different time points (i.e. 15, 30, 60, 90, and 120 min) and replaced with fresh solutions pre-warmed at 37 °C. All BL and AP solutions collected at the end of the transport experiment were stored at - 80 °C prior to analysis. Three independent transport experiments were performed, each in duplicate.

2.3.4. HPLC-Chip-MS/MS analysis

HPLC-Chip MS analysis of absorbed peptides was performed according to a previously published method (Lammi et al., 2016), as reported in Supplementary material. The raw files obtained from the MS analyzer were processed by Spectrum Mill MS Proteomics Workbench (Rev B.04.00, Agilent). The extraction of MS/MS spectra was conducted accepting a minimum sequence length of 3 amino acids and merging scans with same precursor within a mass window of \pm 0.4 *m/z* in a time frame of \pm 5 s. Trypsin or pepsin were chosen as digestive enzymes; 2 missed cleavage were allowed. MS/MS search was conducted against the subset of *C. sativa* protein sequences (47576 entries) downloaded from UNIProtKB (<http://www.uniprot.org/>). The mass tolerance of parent and fragments of MS/MS data search was set at 1.0 Da for the precursor ions and 0.7 for fragment ions respectively. Threshold used for peptide identification score \geq 8; Scored Peak Intensity SPI% \geq 70%; Local False Discovery Rate \leq 0.1%.

2.4. Antioxidant activity of hempseed peptides

2.4.1. 1-Diphenyl-2-picrylhydrazyl radical (DPPH) assay

The DPPH assay was performed by a standard method with a slight modification. Briefly, 45 μ L of 0.0125 mM DPPH solution (dissolved in methanol) was added to 15 μ L of the HP hydrolysate and lysates of pre-treated cells at the final concentrations of 0.50, 1.0, and 2.50 mg/mL, whereas the single peptides H2 and H3 were tested at the final concentrations of 10 up to 200 μ M. The reaction for scavenging the DPPH radicals was performed in the dark at room temperature and the absorbance was measured at 520 nm after 30 min incubation.

2.4.2. 2,2'-Azino-bis(3-ethylbenzothiazoline-6-sulfonic) acid diammonium salt assay

The Trolox equivalent antioxidant capacity (TEAC) assay is based on the reduction of the 2,2'-azino-bis(3-ethylbenzothiazoline-6-sulfonic) acid (ABTS) radical induced by antioxidants. The ABTS radical cation (ABTS⁺) was prepared by mixing a 7 mM ABTS solution (Sigma-Aldrich, Milan, Italy) with 2.45 mM potassium persulfate (1:1) and stored for 16 h at room temperature and in dark. To prepare the ABTS reagent, the ABTS⁺ was diluted in 5 mM phosphate buffer (pH 7.4) to obtain a stable absorbance of 0.700 (\pm 0.02) at 730 nm. For the assay, 10

μ L of H2 and H3 peptides at the final concentrations of 10, 2, 50, 100, and 200 μ M were added to 140 μ L of diluted the ABTS⁺. The microplate was incubated for 30 min at 30 °C and the absorbance was read at 730 nm using a microplate reader Synergy H1 (Biotek). The TEAC values were calculated using a Trolox (Sigma-Aldrich, Milan, Italy) calibration curve (60–320 μ M).

2.4.3. FRAP assay

The FRAP assay evaluates the ability of a sample to reduce ferric ion (Fe³⁺) into ferrous ion (Fe²⁺). Thus, 10 μ L of H2 and H3 peptides at the final concentrations of 10, 25, 5, 100, and 200 μ M were mixed with 140 μ L of FRAP reagent. The FRAP reagent was prepared by mixing 1.3 mL of a 10 mM TPTZ (Sigma-Aldrich, Milan, Italy) solution in 40 mM HCl, 1.3 mL of 20 mM FeCl₃ \times 6 H₂O and 13 mL of 0.3 M acetate buffer (pH 3.6). The microplate was incubated for 30 min at 37 °C and the absorbance was read at 595 nm. The results were calculated by a Trolox (Sigma-Aldrich, Milan, Italy) standard curve obtained using different concentrations (3–400 μ M). Absorbances were recorded on a microplate reader Synergy H1 (Biotek).

2.4.4. ORAC assay

The ORAC assay is based on the scavenging of peroxy radicals generated by the azo 2,2'-azobis(2-methylpropionamide) dihydrochloride (AAPH, Sigma-Aldrich, Milan, Italy). Briefly, 25 μ L of H2 and H3 peptides were added to 50 μ L sodium fluorescein (2.934 mg/L) at the final concentrations of 10, 25, 50, 100, and 200 μ M (Sigma-Aldrich, MO, USA) and incubated for 15 min at 37 °C. Then, 25 μ L of AAPH (60.84 mM) were added and the decay of fluorescein was measured at its maximum emission of 528/20 nm every 5 min for 120 min using a microplate reader Synergy H1 (Biotek). The area under the curve (AUC) was calculated for each sample subtracting the AUC of the blank. The results were calculated using a Trolox calibration curve (2–50 μ M).

2.5. Antioxidant activity of hempseed peptides on HepG2 cells

2.5.1. HepG2 cell culture conditions

Human hepatic HepG2 cells and intestinal Caco-2 cells were cultured in DMEM high glucose with stable L-glutamine, supplemented with 10% FBS, 100 U/mL penicillin, 100 μ g/mL streptomycin (complete growth medium) with incubation at 37 °C under 5% CO₂ atmosphere.

2.5.2. 3-(4,5-Dimethylthiazol-2-yl)-2,5-diphenyltetrazolium bromide (MTT) assay

A total of 3×10^4 HepG2 cells/well were seeded in 96-well plates and treated with peptides H2 and H3 (from 1 μ M to 1 mM) or vehicle (H₂O) in complete growth media for 48 h at 37 °C under 5% CO₂ atmosphere. Subsequently, the solvent was aspirated and 100 μ L/well of filtered 3-(4,5-dimethylthiazol-2-yl)-2,5-diphenyltetrazolium bromide (MTT) solution added. After 2 h of incubation at 37 °C under 5% CO₂ atmosphere, 0.5 mg/mL solution was aspirated and 100 μ L/well of the lysis buffer (8 mM HCl + 0.5% NP-40 in DMSO) were added. After 10 min of slow shaking, the absorbance at 575 nm was read on the microplate reader Synergy H1 (Biotek)

2.5.3. Fluorometric intracellular ROS assay

For cells preparation, 3×10^4 HepG2 cells/well were seeded on a black 96-well plate overnight in growth medium. The day after, the medium was removed, 50 μ L/well of Master Reaction Mix was added and the cells were incubated at 5% CO₂, 37 °C for 1 h in the dark. Then, the HP hydrolysate and peptides H2 and H3 were added to reach the final concentrations of 0.5 and 1.0 mg/mL (HP), 100.0 μ M (H2) and 25.0 μ M (H3), respectively, and incubated at 37 °C for 24 h. To induce ROS, cells were treated with H₂O₂ at a final concentration of 1.0 mM for 30 min at 37 °C in the dark and fluorescence signals (ex./em. 490/525 nm) were recorded using a microplate reader Synergy H1 (Biotek).

2.5.4. Lipid peroxidation (MDA) assay

HepG2 cells (2.5×10^5 cells/well) were seeded in a 24 well plate and, the following day, they were treated with H2 (100 μ M) and H3 (25.0 μ M) peptides for 24 h at 37 °C under 5% CO₂ atmosphere. The day after, cells were incubated with H₂O₂ 1 mM or vehicle (H₂O) for 1 h, then collected and homogenized in 150 μ L ice-cold MDA lysis buffer containing 3 μ L of butylated hydroxytoluene (BHT) (100 \times). Samples were centrifuged at 13,000 g for 10 min, then were filtered through a 0.2 μ m filter to remove insoluble material. To form the MDA-TBA adduct, 300 μ L of the TBA solution were added into each vial containing 100 μ L samples and incubated at 95 °C for 60 min, then cooled to RT for 10 min in an ice bath. For analysis, 100 μ L of each reaction mixture were pipetted into a clear 96 well plate and the absorbance were measured at 532 nm using the microplate reader Synergy H1 (Biotek). To normalize the data, total proteins for each sample were quantified by Bradford method.

2.5.5. Nitric oxide (NO) level evaluation on HepG2 cells

HepG2 cells (1.5×10^5 /well) were seeded on a 24-well plate. The next day, cells were treated with H2 and H3 peptides to reach the final concentrations of 100 μ M (H2) and 25 μ M (H3) and incubated at 37 °C under a 5% CO₂ atmosphere for 24 h. After incubation, cells were treated with H₂O₂ (1.0 mM) or vehicle (H₂O) for 1 h, then the cell culture media were collected and centrifuged at 13,000 g for 15 min to remove insoluble material. The NO determination was carried out by Griess test. Briefly, 1.0 g of Griess reagent powder were solved in 25.0 mL of distilled H₂O and 50 μ L of the solution were incubated with 50 μ L of the culture supernatants for 15 min at RT in the dark. The absorbance was measured at 540 nm using the microplate reader Synergy H1 (Biotek).

2.5.6. iNOS and Nrf-2 protein level evaluation by western blot analysis

A total of 1.5×10^5 HepG2 cells/well were seeded on 24-well plates and incubated at 37 °C under a 5% CO₂ atmosphere. The following day, cells were treated with 100 μ M of H2, 25.0 μ M of H3 peptides or vehicle (H₂O) in a complete growth medium for 24 h. The day after, cells were treated with H₂O₂ (1.0 mM) or vehicle (H₂O) for 1 h. After each treatment, cells were scraped in 30 μ L ice-cold lysis buffer [RIPA buffer + inhibitor cocktail + 1:100 PMSF + 1:100Na-orthovanadate] and transferred in an ice-cold microcentrifuge tube. After centrifugation at 13,300 g for 15 min at 4 °C, the supernatant was recovered and transferred into a new ice-cold tube. Total proteins were quantified by the Bradford method and 50 μ g of total proteins loaded on a precast 7.5% sodium dodecyl sulfate - polyacrylamide gel (SDS-PAGE) at 130 V for 45 min. Subsequently, the gel was pre-equilibrated with 0.04% SDS in H₂O for 15 min at RT and transferred to a nitrocellulose membrane (Mini nitrocellulose Transfer Packs, Bio-Rad) using a trans-Blot Turbo (Bio-Rad) at 1.3 A, 25 V for 7 min. On milk or BSA blocked membrane, target proteins were detected by primary antibodies as follows: anti-iNOS, anti-Nrf-2 and anti- β -actin. Secondary antibodies conjugated with HRP and a chemiluminescent reagent were used to visualize target proteins and their signal was quantified using the Image Lab Software (Bio-Rad). The internal control β -actin was used to normalize loading variations.

2.6. Statistical analysis

All the data sets were checked for normal distribution by D'Agostino and Pearson test. Since they are all normally distributed with p-values < 0.05, we proceeded with statistical analyses by One-Way ANOVA followed by Tukey's post-hoc tests and using GraphPad Prism 9 (San Diego, CA, USA). Values were reported as means \pm standard deviation (s.d.); p-values < 0.05 were considered to be significant.

3. Results & discussion

3.1. Antioxidant activity of HP hydrolysate

To evaluate the radical scavenging activity of the HP hydrolysate, the DPPH assay was employed, since this test is widely applied to test the ability of natural compounds to act as free radical scavengers or hydrogen donors (Kedare & Singh, 2011). The hydrolysate was tested in the range from 0.5 to 2.5 mg/mL. The results (Fig. 1A) clearly suggest that this hydrolysate scavenges the DPPH radical with a dose-response trend. In detail, it reduces the DPPH radicals by $16.9 \pm 5.4\%$, $25.8 \pm 3.8\%$, and $50.7 \pm 7.8\%$, respectively, at 0.5, 1.0, and 2.5 mg/mL (Fig. 1A). Even though, the radical scavenging activity of food protein hydrolysates is influenced by many factors (such as the proteases used for the generation of the hydrolysates, the size and amino acid composition of the obtained peptides, and the DPPH assay conditions), our results suggest that HP hydrolysate is more active than other hempseed protein hydrolysate, obtained by co-digesting the proteins with pepsin and pancreatin, which are poor scavengers of DPPH, i.e. about 4% at 1 mg/mL (Girgih, Udenigwe, & Aluko, 2011). These different behaviors may be explained considering that the extensive protein hydrolysis obtained by the combination of pepsin and pancreatin probably impairs the antioxidant activity. Indeed, HP hydrolysate is 6.5-fold a more potent DPPH radical scavenger than the hydrolysate obtained by co-digesting the hempseed proteins with pepsin and pancreatin. Moreover, HP hydrolysate is also a more active radical scavenger than a soybean protein hydrolysate obtained with the same enzyme (Lammi, Bollati, & Arnoldi, 2019).

In light with these pieces of evidence, the assessment of the ability of HP hydrolysate to scavenge the DPPH radicals was carried out also at cellular levels. More in details, HepG2 cells were treated with HP hydrolysate in the 0.5–2.5 mg/mL range of concentrations. After 24 h, cells were lysated and the DPPH assay was performed. In line with the previous results, our findings suggest that HP hydrolysate reduces the DPPH radical by $14.8 \pm 5.6\%$, $22.9 \pm 14.9\%$, and $56.6 \pm 8.4\%$, respectively, at 0.5, 1.0, and 2.5 mg/mL.

Based on these results, to evaluate whether the HP hydrolysate modulates the H₂O₂-induced ROS production, HepG2 cells were pre-treated with it (0.5 and 1.0 mg/mL) overnight at 37 °C. The following day, the same cells were treated with 1 mM H₂O₂ for 30 min at 37 °C. Results (Fig. 2) clearly suggest that the treatment of HepG2 cells with H₂O₂ alone produces a significant augmentation of intracellular ROS levels by $153.3 \pm 5.6\%$ versus the control cells, which was attenuated by the pre-treatment with the HP hydrolysate that reduced the H₂O₂-induced intracellular ROS by $14.1 \pm 6.7\%$ at 0.5 mg/mL. Interestingly, at 1 mg/mL, the HP hydrolysate reduces the ROS level by $72.1 \pm 5.0\%$ under basal conditions even in presence of H₂O₂ stimulation, confirming that it can act as a natural antioxidant. These results are in line with the effect of peptic soybean peptides in the modulation of intracellular ROS levels after the H₂O₂ stimulation of HepG2 cells (Lammi et al., 2019).

3.2. Trans-epithelial transport of HP hydrolysate using differentiated Caco-2 cells

Differentiated Caco-2 cells were incubated with the HP hydrolysate in the AP compartments at a 1 mg/mL concentration. After 4 h treatment, the AP and BL media were collected and submitted to HPLC-Chip-MS/MS analysis. For monitoring cell monolayer permeability and excluding non-specific peptide passage, TEER measurements were taken at the beginning and end of each experiment. Moreover, phenol-red passage across the monolayer was assayed at the experiment end (Ferruzza, Scarino, Gambling, Natella, & Sambuy, 2003). Both assays demonstrated that the incubation with the HP hydrolysate did not affect monolayer permeability (data not shown). Only filters showing TEER values and a phenol red passage similar to untreated control cells were considered for peptide transport analysis. The starting peptic peptide

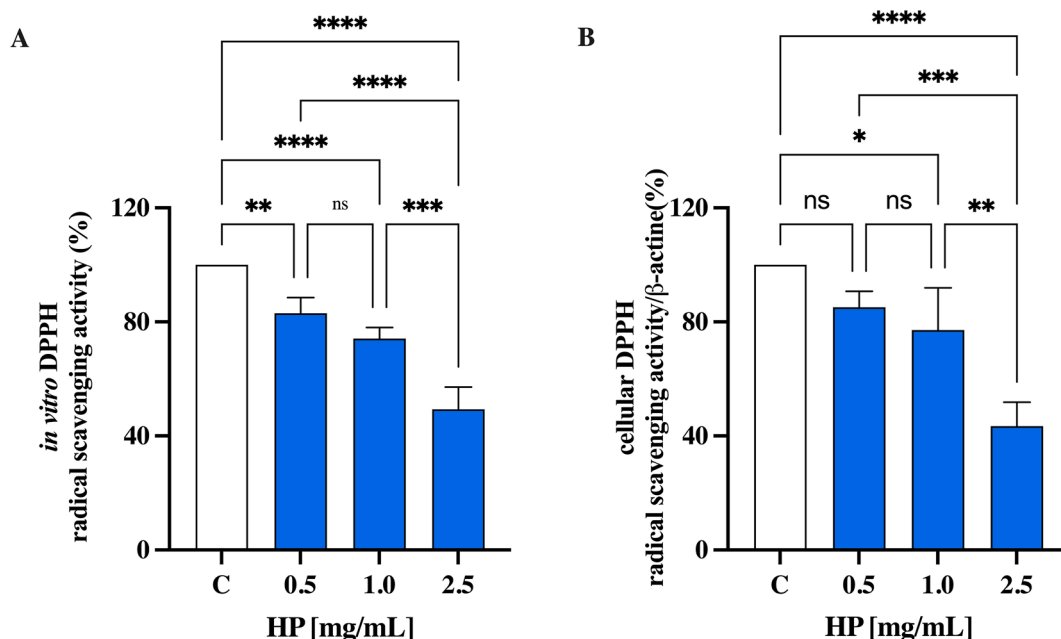


Fig. 1. Chemical (A) and cellular (HepG2, B) DPPH radical scavenging activity of HP hydrolysate. The data points represent the averages \pm s.d. of four independent experiments in duplicate. C: control sample. (*) $p < 0.05$, (**) $p < 0.01$, (***) $p < 0.001$, (****) $p < 0.0001$.

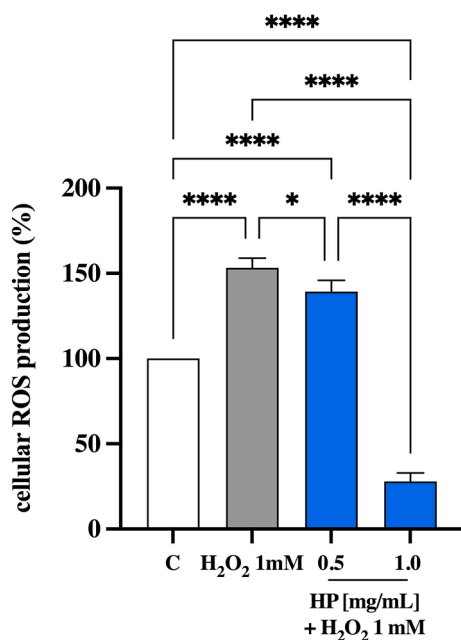


Fig. 2. Effects of HP on the modulation of H₂O₂-induced ROS levels in HepG2 cells. HP reduce the H₂O₂ (1 mM)-induced ROS levels in HepG2 cells. Data represent the mean \pm s.d. of six independent experiments performed in triplicate. All data sets were analyzed by One-way ANOVA followed by Tukey's post-hoc test. C: control sample. (*) $p < 0.05$, (****) $p < 0.0001$.

mixture and the AP and BL samples taken at the end of transport experiments were analyzed by HPLC-Chip-MS/MS. Fig. S1 (Supplementary material) shows exemplary chromatographic profiles of AP and BL peptides, which were identified through MS/MS ion search, using the SpectrumMill search engine.

Table 1 shows the peptides identified in the starting hydrolysate as well as in the AP and/or BL samples. Notably, among the peptides present in the starting HP hydrolysate, only five peptides were able to cross the mature Caco-2 cells. Out of these five absorbed species, H1

belongs to Edestin 3 (A0A219D2X4), H2, H4, and H5 to Edestin1 (A0A090CXP7), whereas H3 belongs to Cytochrome c biogenesis protein CcsA (A0A0U2DTB8). H4 is the longest absorbed peptide with 12 amino acids residues within its sequence, whereas H3 and H5 are the shortest ones, accounting for 8 amino acid residues. Finally, H1 and H2 have 10 and 9 amino acid residue sequences, respectively. Moreover, H1 and H4 are absorbed by Caco-2 cells and are not degraded by the action of the peptidases, which are expressed at the AP side of the differentiated cells during incubation, whereas some other peptides, i.e. H2 and H5, are transported by Caco-2 cells but they are degraded during the 4 h of incubation by intestinal peptidase producing other shorter peptide fragments.

Working on a peptide mixture with a complex composition, it is not feasible to characterize the mechanism by which peptides are transported by intestinal cells, since more than one mechanism may occur at the same time during the trans-epithelial transport of the total hydrolysate.

Overall, food derived peptides may be transported across the intestinal brush-border membrane into the bloodstream via one or more of the following routes: (i) peptide transport 1 (PepT1)-mediated route, (ii) paracellular route via tight junctions, (iii) transcytosis route, and (iv) passive transcellular diffusion (Xu, Yan, Zhang, & Wu, 2019). Peptide size, charge, hydrophobicity, and degradation due to the action of peptidases are among the main factors influencing the absorption through one or more of these routes. In general, short peptides, such as dipeptides and tripeptides, are preferentially transported by PepT1, due to its high-capacity, low-affinity, and high expression in intestinal epithelium (Daniel, 2004), whereas highly hydrophobic peptides are transported by simple passive transcellular diffusion or by transcytosis (Miguel et al., 2008). Based on these considerations, the hydrophobicity of all the transported peptides was calculated (see Table 1). The results suggest that these peptides may be preferentially transported by paracellular route and/or by transcytosis.

3.3. Screening of the antioxidant activity of transported hempseed peptides

All peptides detected in the BL samples were synthesized and screened for their antioxidant activity at concentrations ranging from 10

Table 1
LC-ESI-MS/MS based identification of peptic peptides from transport experiments.

	Accession no ^a	m/z ^b (charge)	Observed ^b [M + H] ⁺ (Da)	Expected ^b [M + H] ⁺ (Da)	Peptide sequence ^b	Short name	M ^c	AP ^c	BL ^c	Hydrophobicity (Kcal ^a ·mol ⁻¹) ^d
<i>Peptic hempseed peptides</i>										
Edestin, 3	A0A219D2X4	545,28	1089,568	1089,568	328 DVFSPQAGRL ₃₃₇	H1	+ ^e	+	+	+12.95
Edestin, 1	A0A090CXP7	586.93	986,541	986,541	456WVSPLAGRT ₅₅₈	H2	+	-	+	+8.41
Cytochrome c biogenesis protein CcsA	A0A0U2DTB8	480,80	960,595	960,591	293IGFLIIWV ₃₀₀	H3	-	-	+	+0.18
Edestin, 1	A0A090CXP7	645,81	1291,661	1291,664	341DVFTPQAGRIST ₃₅₂	H4	+	+	+	+13.58
Edestin, 1	A0A090CXP7	434,78	868,524	868,525	461IRALPEAV ₄₆₈	H5	+	-	+	+11.65

^a According to "UniProtKB" (<http://www.uniprot.org/>).

^b The identification of protein parent was performed using SpectrumMill Workbench

^c M, starting peptide mixture of peptic peptides; AP, apical chamber samples; BL, basolateral chamber samples.

^d According to PepDraw (<http://pepdraw.com>).

^e +, detected.

to 200 μ M using the ABTS, DPPH, ORAC, and FRAP assays (Figs. 3 and 2S). H2 and H3 resulted to be the best antioxidant peptides. H2 scavenged the ABTS radical by $147 \pm 7.9\%$, $164.2 \pm 1.1\%$, $174.1 \pm 0.4\%$, $178.8 \pm 0.9\%$, and $179.3 \pm 0.5\%$, whereas H3 by $142.7 \pm 10.3\%$, $146.1 \pm 8.1\%$, $149.6 \pm 5.6\%$, $153.1 \pm 2.5\%$, and $157.5 \pm 3.3\%$, respectively, at 10, 25, 50, 100, and 200 μ M (Fig. 3A, E). H2 scavenged the DPPH radical by $24.8 \pm 0.3\%$, and $33.4 \pm 4.2\%$ and $36.1 \pm 5.2\%$ (Fig. 3B), whereas H3 reduced the DPPH radical by $29.6 \pm 2.2\%$, $29.8 \pm 3.2\%$, $31.8 \pm 3\%$, $33.5 \pm 3.3\%$, and $33.6 \pm 0.6\%$, respectively, at 10, 25, 50, 100, and 200 μ M (Fig. 3F).

In addition, in the ORAC test, H2 was able to scavenge the peroxy radicals generated by 2,2'-azobis(2-methylpropanimidine) dihydrochloride up to $489.4 \pm 56.9\%$, $614.8 \pm 13.3\%$, $678 \pm 52.4\%$, $679.5 \pm 55.6\%$, and $621.8 \pm 44.6\%$, whereas H3 by 148.9 ± 12.1 , 181.8 ± 12.5 , 207.5 ± 13.7 , 331.3 ± 14.5 , and $480.8 \pm 9.0\%$, respectively, at 10, 25, 50, 100, and 200 μ M (Fig. 3C and G). Finally, H2 increased the FRAP by $143.1 \pm 28.2\%$, $144.5 \pm 32.5\%$, $212.6 \pm 31\%$, $298.1 \pm 58.7\%$, and $587.6 \pm 27.3\%$, whereas H3 by $207.5 \pm 23.5\%$, $299.3 \pm 42.8\%$, $355.8 \pm 19.3\%$, $519.5 \pm 13.7\%$, and $782 \pm 6.8\%$ at 10, 25, 50, 100, and 200 μ M, respectively (Fig. 3D and 3H). By performing the same assays, H1, H4, and H5 did not show any significant antioxidant behavior (Fig. 2S).

Many physical-chemical factors may influence the ability of peptides to exert antioxidant activity. In fact, although certain aspects of the structure-function relationship of antioxidant peptides are still poorly understood (Harnedy, O'Keefe, & FitzGerald, 2017), it has been suggested that chain length, amino acid type, amino acid composition, and amino acid sequence, the location of specific amino acids in a peptide chain may be critical issues for exerting the antioxidant property (Gallego, Mora, & Toldra, 2018). In this context, short peptides may be often potent antioxidants.

Literature indicates that, besides containing hydrophobic amino acids, such as Leu or Val, in their N-terminal regions, peptides containing nucleophilic sulfur-containing amino acid residues (Cys and Met), aromatic amino acid residues (Phe, Trp, and Tyr) and/or the imidazole ring-containing His are generally found to possess strong antioxidant properties (Nwachukwu & Aluko, 2018, 2019). Based on these considerations, H3 is the shortest peptide among those tested and it stands out for the presence of two aromatic amino acids (Trp and Phe) within its sequence, which certainly contribute to its antioxidant activity. In addition, since the repetitive di- or tri- amino acid residues within a peptide have been linked to enhanced antioxidant activity (Jin, Liu, Zheng, Wang, & He, 2016), the H3 antioxidant behavior may be linked to the repetitive II sequence.

The antioxidant activity of peptide H2 is linked to the presence of Trp residue located in the N-terminal portion of the peptide as well as to the presence of an Arg residue in the C-terminal. In particular, the Arg residue in C-terminal may be correlated with its high ABTS radical scavenging ability. This evidence is in line with the fact that the C-terminal

Arg residue has been linked to high antioxidant activity of certain peptides, i.e. GLFGPR and GATGPQGPLGPR (Sae-Leaw et al., 2017).

3.4. H2 and H3 decrease the H₂O₂-induced ROS and lipid peroxidation levels in hepatic HepG2 cells

Considering all the results obtained by the previous assays, only H2 and H3 were chosen for a deeper assessment of the antioxidant properties at cellular level, measuring their protective effects after induction of oxidative stress using H₂O₂ on human hepatic HepG2 cells. Before cellular evaluation, however, it was necessary to perform MTT experiments in order to exclude any potential cytotoxic effect. Results suggest that H2 is safe for the hepatic cells at all the doses in the range 1 nM-1 mM, whereas for H3 the highest safe dose for HepG2 cell vitality is 25 μ M (Fig. S3). In addition, any morphological variations of HepG2 cells treated w/o and with H₂O₂ (1 mM) for 1 h and cells pre-treated with both H2 (100 μ M) and H3 (25 μ M) peptides and then treated with H₂O₂ (1 mM) was observed by inverted microscopy (Fig. S4).

Based on the MTT results and on the antioxidant activity evaluation by chemical assays, it was decided to test the H2 and H3 effect on HepG2 cells at the fixed concentrations of 100 and 25 μ M, respectively. The concentration of H2 was selected based on its safety in the MTT assay, whereas that of H3 was the highest safe concentration even if it was not the most active in the antioxidant experiments performed employing ABTS, FRAP, ORAC, and DPPH assays, respectively.

Fig. 4A shows that the treatment of HepG2 cells with H₂O₂ alone produces a significant increase of intracellular ROS levels by $51.7 \pm 5.7\%$, which was attenuated by the pre-treatment with peptides H2 and H3: H2 reduced the ROS by $23.8 \pm 12.5\%$ at 100 μ M, whereas H3 by $23.2 \pm 12.8\%$ at 25 μ M. These findings indicate that both peptides H2 and H3 significantly protected the HepG2 cells from the H₂O₂-induced oxidative stress. Notably, H3 appeared to be 4-fold more effective than H2.

Other food peptides are antioxidant in cellular models. ADWGGPLPH, a wheat germ derived peptide, significantly reduces the intracellular ROS production deriving from hyperglycemia in vascular smooth muscle cells (F. Wang et al., 2020), peptides GPEGPMGLE, EGPFPGPEG, GFIGPTE, from collagen of red-lip croaker, decreases intracellular ROS levels in H₂O₂-treated HepG2 cells (Wang, Zhao, Zhao, Chi, & Wang, 2020), and peptides VEGNLQVLRPR, LAGNPHQQQN, HNLDTQTESDV, AGNDGFYVTLK, QQRQQQL, AELQVVDHLGQTV, EQEEEEESTGRMK, WSVWEQELED, from defatted walnut meal, decrease ROS production in H₂O₂-treated SHSY5Y cells (Sheng et al., 2019).

Lipids of cellular membranes are susceptible to oxidative attack, typically by ROS, resulting in a well-defined chain reaction with the generation of end products, such as malondialdehyde (MDA) and related compounds, known as TBA reactive substances (TBARS). Based on these

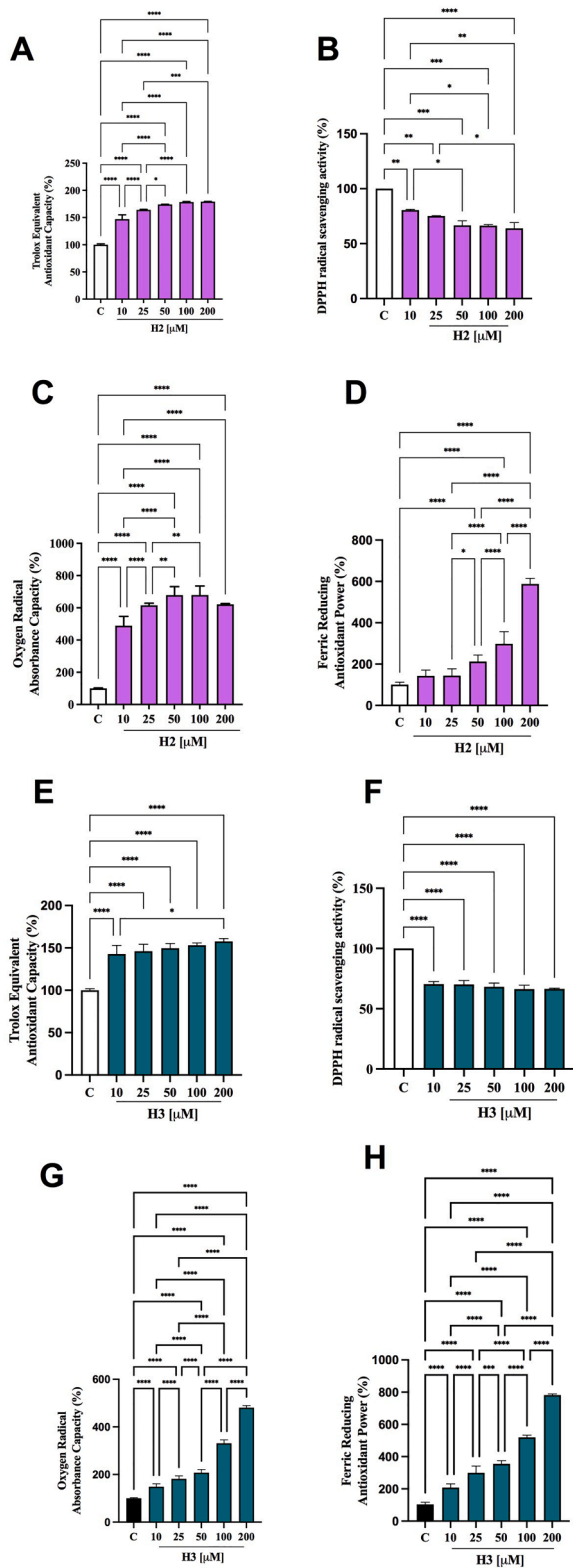


Fig. 3. Antioxidant power evaluation of H2 and H3 peptides by 2,2-azino-bis-(3-ethylbenzothiazoline-6-sulfonic) acid (ABTS) (A, E), 2,2-diphenyl-1-picrylhydrazyl (DPPH) (B, F), oxygen radical absorbance capacity (ORAC) (C, G) and ferric reducing antioxidant power (FRAP) (D, H) assays, respectively. The data points represent the averages \pm s.d. of four independent experiments performed in duplicate. All data sets were analyzed by One-way ANOVA followed by Tukey's post-hoc test. C: control sample. (*) $p < 0.5$; (**) $p < 0.01$; (***) $p < 0.001$; (****) $p < 0.0001$.

considerations, the capacity of H2 and H3 to modulate the H_2O_2 -induced lipid peroxidation in human hepatic HepG2 cells was assessed measuring the reaction of MDA precursor with the TBA reagent to form fluorometric ($\lambda_{ex} = 532/\lambda_{em} = 553$ nm) product, proportional to the amount of TBARS (MDA equivalents) present. In agreement with the observed increase of ROS after the H_2O_2 treatment, a significant increase of the lipid peroxidation was observed up to $135.9 \pm 10.8\%$ at cellular level (Fig. 4B). In addition, the pre-treatment of HepG2 cells with both peptides determined a significant reduction of lipid peroxidation even under basal conditions. Fig. 4B clearly shows that H2 decreases the lipid peroxidation up to $99.5 \pm 14.6\%$ at 100 μ M, whereas H3 up to $91.9 \pm 13.3\%$ at 25 μ M (Fig. 4B). Since the lipid peroxidation is a validated marker of oxidative stress, these findings confirm the effective antioxidant property of hempseed peptides H2 and H3 and that H3 is 4-fold more active than H2 also in reducing intracellular MDA production.

VNP and YGD, two peptides from fermented grain (Jiupei), are able to decrease the MDA levels in AAPH-treated HepG2 cells (Jiang et al., 2019). In addition, QDHCH, a peptide from pine nut protein, reduced MDA content in H_2O_2 -treated HepG2 cells (Liang, Zhang, & Lin, 2017). Finally, IYVVDLR, IYVFVR, VVFVDR, VIYVVDLR are four soybean peptides, which modulate both MDA and ROS level in H_2O_2 -treated Caco-2 cells (Zhang et al., 2019).

3.5. H2 and H3 mediate antioxidant activity through the Nrf-2 pathway modulation

Nuclear factor erythroid 2-related factor 2 (Nrf-2)/antioxidant response elements (ARE) signaling plays a crucial role in the protection against oxidative stress and is responsible for the maintenance of homeostasis and redox balance in cells and tissue. Indeed, the Kelch-like ECH associated protein 1 (Keap1)-Nrf2 signaling pathway is considered one of the plausible antioxidant mechanisms of peptides *in vivo*. Nrf-2 regulates cellular responses against environmental stresses and is bound to Keap1 in the cytoplasm under basal conditions. However, during oxidative stress conditions, Nrf-2 is released from Keap1 and translocated into the nucleus, where it binds to AREs and upregulates target genes, such as superoxide dismutase, catalase and glutathione, that are cellular antioxidant enzymes expected to protect cells from oxidative stress (Saha, Buttari, Panieri, Profumo, & Saso, 2020). To assess the effects of H2 and H3 on the Nrf-2-pathway, western blotting experiments were performed. Our findings indicated that after the treatment of HepG2 cells with H_2O_2 (1 mM), a significant decrease of Nrf-2 protein level by $25.3 \pm 10.8\%$ was observed versus control cells (Fig. 5A-C). The pretreatment with H2 and H3 produce antioxidant activity through the Nrf-2 pathway modulation in H_2O_2 treated HepG2 cells. In facts, H2 increased the Nrf-2 protein levels up to $126.1 \pm 19.7\%$ at 100 μ M (Fig. 5A and 5C), whereas H3 up to $115.4 \pm 12.7\%$ at 25 μ M (Fig. 5 B, C). Statistical analysis confirms that also in this case, H3 is 4-fold more active than H2, since any difference was observed between both peptides (Fig. 5 C). Moreover, it clearly appears that at 100 μ M H2 is able to increase the Nrf-2 protein level more than basal condition (C) even in the presence of H_2O_2 (Fig. 5A and C). Recently, Oryza Peptide-P60 (OP60), a commercial rice peptide, has been reported to increase intracellular glutathione levels and the evaluation of the mechanisms underlying the antioxidant potential of this peptide in HepG2 cells suggests that OP60 reduced the oxidant stress induced by H_2O_2 via the Nrf-2 signaling pathway (Moritani et al., 2020).

3.6. H2 and H3 modulate the H_2O_2 -induced NO level production via the iNOS protein modulation in HepG2 cells

Imbalanced ROS levels not only do impair the stability of intracellular macromolecules (such as DNA, proteins, and lipids) but also may react with NO leading to the production of peroxynitrite ($ONOO^-$), which reduces the bioavailability of NO, which is a potent vasorelaxant signaling messenger in vascular system (Beckman, 1996; Shi et al.,

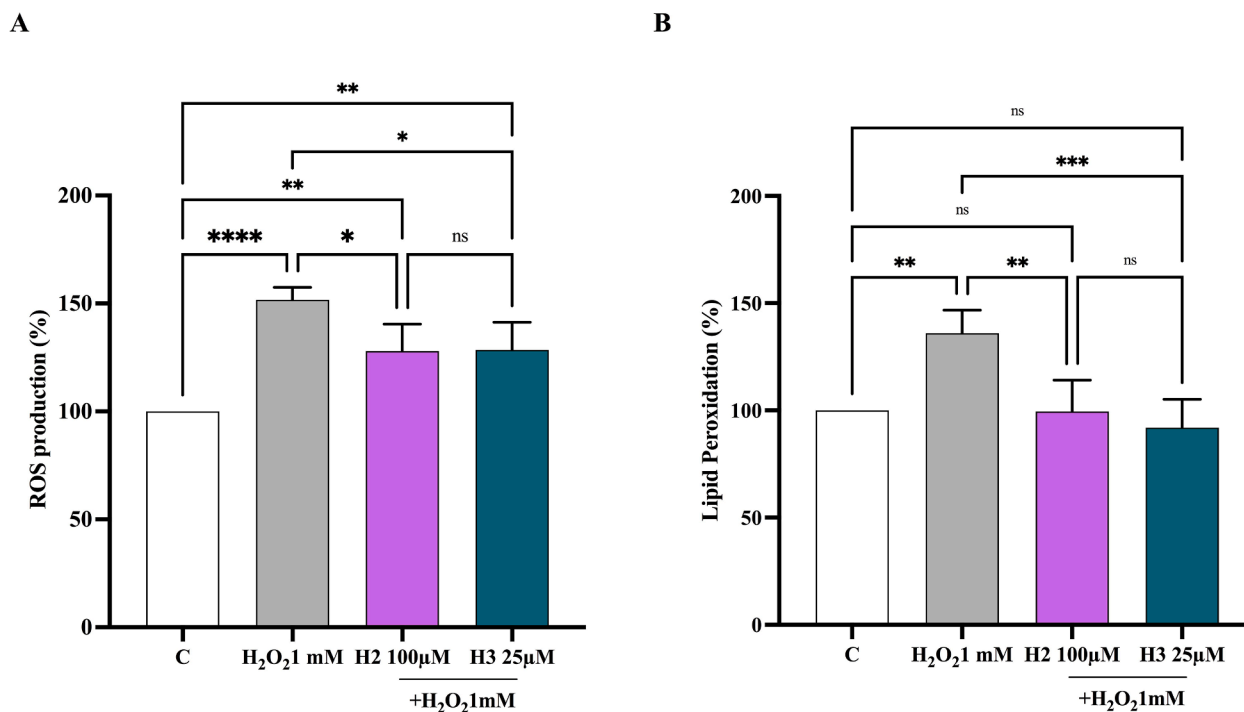


Fig. 4. H2 and H3 peptides reduce the H₂O₂ (1 mM)-induced ROS levels in HepG2 cells (A). H2 and H3 peptides decrease the lipid peroxidation in the same cells after oxidative stress induction by H₂O₂ (B). Data represent the mean \pm s.d. of six independent experiments performed in triplicate. All the data sets were analyzed by One-way ANOVA followed by Tukey's post-hoc test. C: control sample; ns: not significant. (*) $p < 0.5$; (**) $p < 0.01$; (***) $p < 0.001$; (****) $p < 0.0001$.

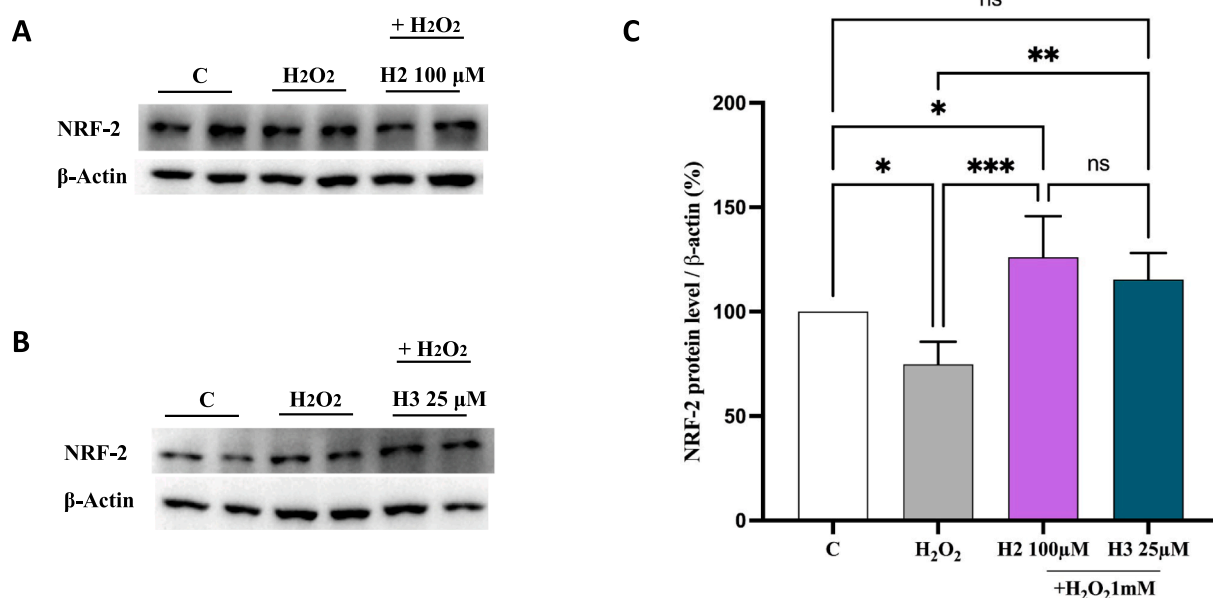


Fig. 5. Effect of H2 (A, C) and H3 (B, C) peptides on the H₂O₂ (1 mM)-induced Nrf-2 levels in human hepatic HepG2 cells. The data points represent the averages \pm s.d. of six independent experiments in duplicate. All data sets were analyzed by One-way ANOVA followed by Tukey's post-hoc test. C: control sample; ns: not significant; (*) $p < 0.5$, (**) $p < 0.01$, (***) $p < 0.001$.

2004). Increased oxidative stress and its downstream effects can lead to various conditions such as cardiovascular diseases (D'Orta et al., 2020).

Based on these considerations, the effects of both H2 and H3 on NO production were evaluated on human hepatic HepG2 cells after oxidative stress induction. Notably, H₂O₂ (1 mM) treatment induced an oxidative stress that led to an increase of intracellular NO levels up to $110 \pm 3.9\%$ (Fig. 6A). Pre-treatment with H2 and H3 reduced the H₂O₂-induced NO overproduction, reducing their values closer than the basal

levels (Fig. 6A). In particular, H2 reduced the NO overproduction up to $96.2 \pm 0.8\%$, whereas H3 up to $105.1 \pm 1.2\%$.

iNOS, is an enzyme expressed in different cell types (Soskić et al., 2011) and it is usually induced during inflammatory events (Habib & Ali, 2011). The generation of NO by iNOS is associated with the alteration of NO homeostasis, which is linked to many pathophysiological conditions. In this study, the effect of H2 and H3 on iNOS protein levels was assessed after oxidative stress induction by western blot

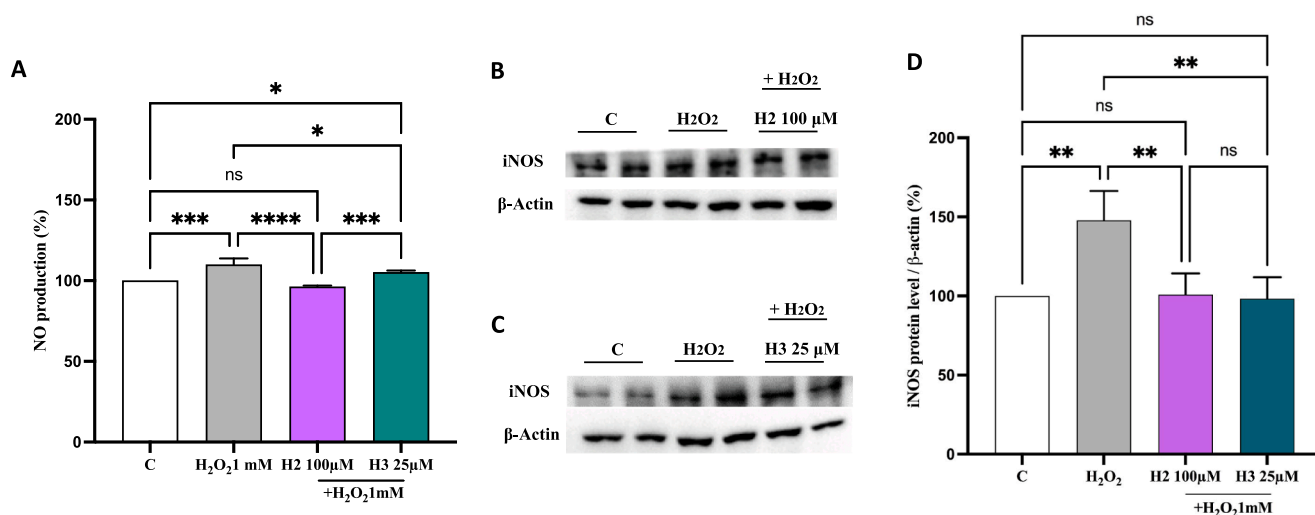


Fig. 6. Effect of H2 and H3 peptides on the H₂O₂ (1 mM)-induced NO production (A) and inducible nitric oxide synthase (iNOS) protein levels (B–D) in human hepatic HepG2 cells. The data points represent the averages ± s.d. of six independent experiments in duplicate. All data sets were analyzed by One-way ANOVA followed by Tukey’s post-hoc test. C: control sample; ns: not significant; (**) p < 0.01.

experiments, in which the iNOS protein band at 130 kDa was detected and quantified (Fig. 6 B–D). Results suggest that after H₂O₂ treatment (1 mM), the iNOS protein increased up to 147.8 ± 18.6% in HepG2 cells. In agreement with the modulation of NO production, pre-treatment of HepG2 cells with both peptides reduced the H₂O₂-induced iNOS protein, bringing their levels close to basal conditions. In particular, H2 reduced the iNOS levels up to 100.9 ± 13.3% at 100 μM (Fig. 6 B, D), whereas H3

reduced up to 98.3 ± 13.6% at 25 μM (Fig. 6 C, D).

Recent pieces of evidence suggest that many bioactive peptides from different food sources exert both antioxidants and anti-inflammatory activities through the modulation of NO levels via iNOS pathway regulation after oxidative stress induction (Zhu et al., 2020), suggesting a potential interplay of both antioxidant and anti-inflammatory activities exerted by these two peptides.

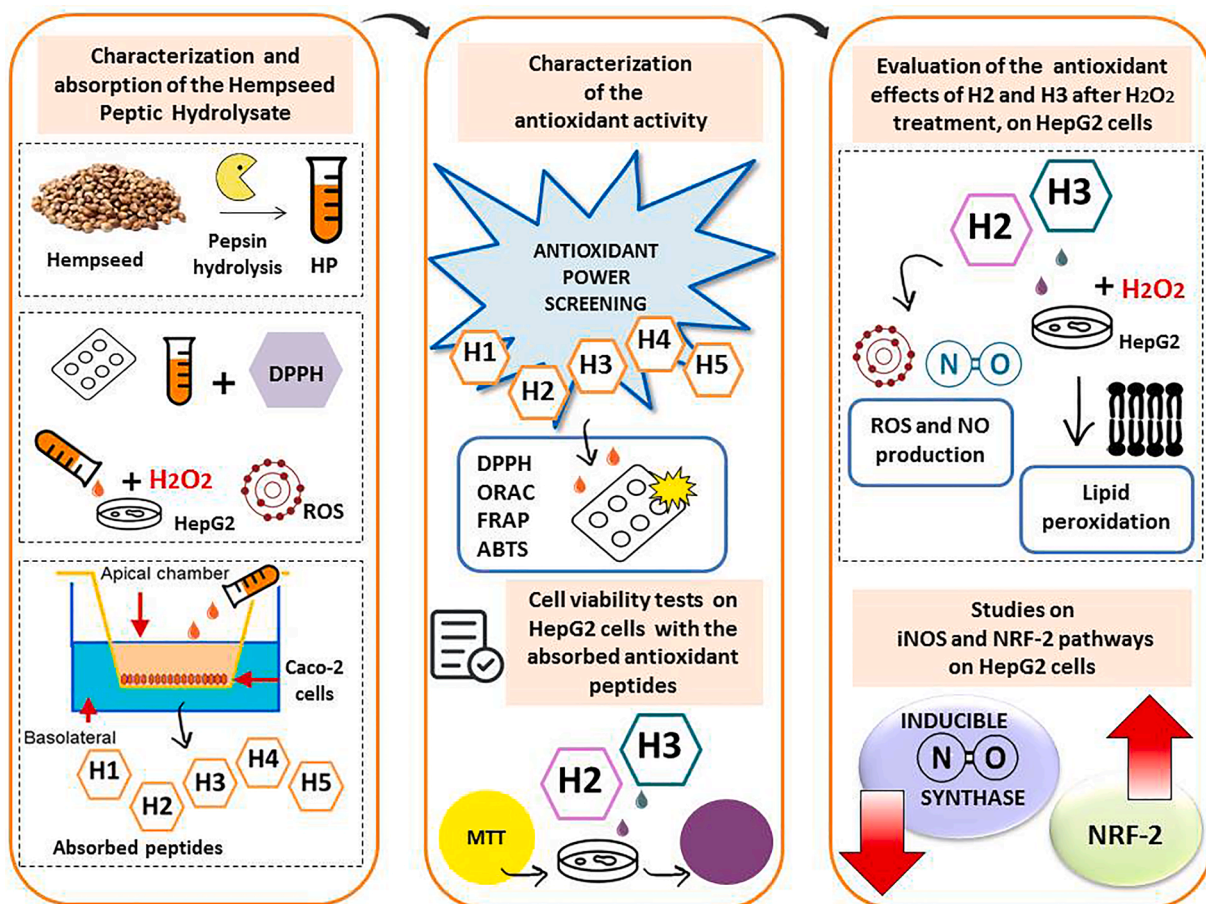


Fig. 7. Flow chart which summarizes the strategy of the work.

4. Conclusions

Antioxidant peptides are considered new useful tools for the prevention and treatment of multifactorial disease in which oxidative stress plays a relevant role. Whereas most published studies on antioxidant peptides restrain the evaluation to the application of chemical assays, here an integrated approach was applied that allowed the identification of two bioavailable hempseed peptides that are able to exert their antioxidant activity also in HepG2 cells where the oxidative stress had been induced by a H₂O₂ treatment (Fig. 7). Overall, our strategy focuses on the use of differentiated Caco-2 monolayer as a “natural sieve of bioavailable species”, which permits to identify few hempseed absorbable peptides, whose antioxidant activity was investigated *in vitro* by using chemical and cell-based techniques. Indeed, this strategy permits to overcome the very crucial issue of bioavailability and the combination of *in vitro* biochemical and cellular assays represents a suitable approach for reducing the *in vivo* assays, which involve high costs and arise ethical issues for the excessive use of animals for routine research.

CRedit authorship contribution statement

Carlotta Bollati: Investigation, Formal analysis. **Ivan Cruz-Chamorro:** Investigation. **Gilda Aiello:** Investigation. **Jianqiang Li:** Investigation. **Guillermo Santos-Sánchez:** Investigation. **Giulia Ranaldi:** Investigation. **Simonetta Ferruzza:** Investigation. **Yula Sambuy:** Writing – review & editing. **Anna Arnoldi:** Funding acquisition, Writing – review & editing. **Carmen Lammi:** Conceptualization, Data curation, Formal analysis, Investigation, Supervision, Writing – original draft, Writing – review & editing.

Declaration of Competing Interest

The authors declare that they have no known competing financial interests or personal relationships that could have appeared to influence the work reported in this paper.

Acknowledgement

We are indebted to Carlo Sirtori Foundation (Milan, Italy) for having provided part of equipment used in this experimentation.

Appendix A. Supplementary material

Supplementary data to this article can be found online at <https://doi.org/10.1016/j.foodres.2021.110720>.

References

Beckman, J. S. (1996). Oxidative damage and tyrosine nitration from peroxynitrite. *Chemical Research in Toxicology*, 9(5), 836–844. <https://doi.org/10.1021/cx9501445>.

Callaway, J. C. (2004). Hempseed as a nutritional resource: An overview. *Euphytica*, 140(1–2), 65–72. <https://doi.org/10.1007/s10681-004-4811-6>.

D’Oria, R., Schipani, R., Leonardini, A., Natalicchio, A., Perrini, S., Cignarelli, A., ... Giorgino, F. (2020). The role of oxidative stress in cardiac disease: from physiological response to injury factor. *Oxidative Medicine and Cellular Longevity*, 2020, 1–29. <https://doi.org/10.1155/2020/5732956>.

Daniel, H. (2004). Molecular and integrative physiology of intestinal peptide transport. *Annual Review of Physiology*, 66(1), 361–384. <https://doi.org/10.1146/annurev.physiol.66.032102.144149>.

Farinon, B., Molinari, R., Costantini, L., & Merendino, N. (2020). The seed of industrial hemp. *Nutrients*, 12(7). <https://doi.org/10.3390/nu12071935>.

Ferruzza, S., Rossi, C., Sambuy, Y., & Scarino, M. L. (2013). Serum-reduced and serum-free media for differentiation of Caco-2 cells. *ALTEX*, 30(2), 159–168. <https://doi.org/10.14573/altex.2013.2.159>.

Ferruzza, S., Scarino, M. L., Gambling, L., Natella, F., & Sambuy, Y. (2003). Biphasic effect of iron on human intestinal Caco-2 cells: Early effect on tight junction permeability with delayed onset of oxidative cytotoxic damage. *Cellular and Molecular Biology (Noisy-le-grand)*, 49(1), 89–99.

Gallego, M., Mora, L., & Toldra, F. (2018). Characterisation of the antioxidant peptide AEEYPPDL and its quantification in Spanish dry-cured ham. *Food Chemistry*, 258, 8–15. <https://doi.org/10.1016/j.foodchem.2018.03.035>.

Girgih, A. T., He, R., & Aluko, R. E. (2014). Kinetics and molecular docking studies of the inhibitions of angiotensin converting enzyme and renin activities by hemp seed (*Cannabis sativa* L.) peptides. *Journal of Agricultural and Food Chemistry*, 62(18), 4135–4144. <https://doi.org/10.1021/jf5002606>.

Girgih, A. T., He, R., Malomo, S., Offengenden, M., Wu, J., & Aluko, R. E. (2014). Structural and functional characterization of hemp seed (*Cannabis sativa* L.) protein-derived antioxidant and antihypertensive peptides. *Journal of Functional Foods*, 6, 384–394. <https://doi.org/10.1016/j.jff.2013.11.005>.

Girgih, A. T., Udenigwe, C. C., & Aluko, R. E. (2011). In Vitro Antioxidant Properties of Hemp Seed (*Cannabis sativa* L.) Protein Hydrolysate Fractions. *Journal of the American Oil Chemists Society*, 88(3), 381–389. <https://doi.org/10.1007/s11746-010-1686-7>.

Habib, S., & Ali, A. (2011). Biochemistry of nitric oxide. *Indian Journal of Clinical Biochemistry*, 26(1), 3–17. <https://doi.org/10.1007/s12291-011-0108-4>.

Harnedy, P. A., O’Keefe, M. B., & FitzGerald, R. J. (2017). Fractionation and identification of antioxidant peptides from an enzymatically hydrolysed *Palmaria palmata* protein isolate. *Food Research International*, 100, 416–422. <https://doi.org/10.1016/j.foodres.2017.07.037>.

Jiang, Y., Zhao, D., Sun, J., Luo, X., Li, H., Sun, X., & Zheng, F. (2019). Analysis of antioxidant effect of two tripeptides isolated from fermented grains (Jiupei) and the antioxidative interaction with 4-methylguaiacol, 4-ethylguaiacol, and vanillin. *Food Science & Nutrition*, 7(7), 2391–2403. <https://doi.org/10.1002/fsn3.2019.7.issue-710.1002/fsn3.1100>.

Jin, D. X., Liu, X. L., Zheng, X. Q., Wang, X. J., & He, J. F. (2016). Preparation of antioxidative corn protein hydrolysates, purification and evaluation of three novel corn antioxidant peptides. *Food Chemistry*, 204, 427–436. <https://doi.org/10.1016/j.foodchem.2016.02.119>.

Kedare, S. B., & Singh, R. P. (2011). Genesis and development of DPPH method of antioxidant assay. *Journal of Food Science and Technology*, 48(4), 412–422. <https://doi.org/10.1007/s13197-011-0251-1>.

Lammi, C., Aiello, G., Boschin, G., & Arnoldi, A. (2019). Multifunctional peptides for the prevention of cardiovascular diseases: A new concept in the area of bioactive food-derived peptides. *Journal of Functional Foods*, 55, 135–145. <https://doi.org/10.1016/j.jff.2019.02.016>.

Lammi, C., Aiello, G., Vistoli, G., Zannoni, C., Arnoldi, A., Sambuy, Y., ... Ranaldi, G. (2016). A multidisciplinary investigation on the bioavailability and activity of peptides from lupin protein. *Journal of Functional Foods*, 24, 297–306. <https://doi.org/10.1016/j.jff.2016.04.017>.

Lammi, C., Bollati, C., & Arnoldi, A. (2019). Antioxidant activity of soybean peptides on human hepatic HepG2 cells. *Journal of Food Bioactives*, 7(2019).

Lammi, C., Bollati, C., Gelain, F., Arnoldi, A., & Pugliese, R. (2019). Enhancement of the stability and anti-DPPIV activity of hempseed hydrolysates through self-assembling peptide-based hydrogels. *Frontiers in Chemistry*, 6. <https://doi.org/10.3389/fchem.2018.0067010.3389/fchem.2018.00670.s001>.

Liang, R., Zhang, Z. M., & Lin, S. Y. (2017). Effects of pulsed electric field on intracellular antioxidant activity and antioxidant enzyme regulating capacities of pine nut (*Pinus koraiensis*) peptide QDHCH in HepG2 cells. *Food Chemistry*, 237, 793–802. <https://doi.org/10.1016/j.foodchem.2017.05.144>.

Malomo, S. A., & Aluko, R. E. (2016). In vitro acetylcholinesterase-inhibitory properties of enzymatic hemp seed protein hydrolysates. *Journal of the American Oil Chemists Society*, 93(3), 411–420. <https://doi.org/10.1007/s11746-015-2779-0>.

Malomo, S. A., Onuh, J. O., Girgih, A. T., & Aluko, R. E. (2015). Structural and antihypertensive properties of enzymatic hemp seed protein hydrolysates. *Nutrients*, 7(9), 7616–7632. <https://doi.org/10.3390/nu7095358>.

Miguel, M., Davalos, A., Manso, M. A., de la Pena, G., Lasuncion, M. A., & Lopez-Fandino, R. (2008). Transepithelial transport across Caco-2 cell monolayers of antihypertensive egg-derived peptides. PepT1-mediated flux of Tyr-Pro-Ile. *Molecular Nutrition & Food Research*, 52(12), 1507–1513. <https://doi.org/10.1002/mnfr.200700503>.

Moritani, C., Kawakami, K., Shimoda, H., Hatanaka, T., Suzuki, E., & Tsuboi, S. (2020). Protective effects of rice peptide oryza peptide-P60 against oxidative injury through activation of Nrf2 signaling pathway in vitro and in vivo. *ACS Omega*, 5(22), 13096–13107. <https://doi.org/10.1021/acsomega.0c01016>.

Nwachukwu, I. D., & Aluko, R. E. (2018). Antioxidant properties of flaxseed protein hydrolysates: influence of hydrolytic enzyme concentration and peptide size. *Journal of the American Oil Chemists Society*, 95(8), 1105–1118. <https://doi.org/10.1002/aocs.12042>.

Nwachukwu, I. D., & Aluko, R. E. (2019). Structural and functional properties of food protein-derived antioxidant peptides. *Journal of Food Biochemistry*, 43(1), e12761. <https://doi.org/10.1111/jfbc.12761>.

Rodriguez-Martin, N. M., Toscano, R., Villanueva, A., Pedroche, J., Millan, F., Montserrat-de la Paz, S., & Millan-Linares, M. C. (2019). Neuroprotective protein hydrolysates from hemp (*Cannabis sativa* L.) seeds. *Food & Function*, 10(10), 6732–6739. <https://doi.org/10.1039/c9fo01904a>.

Sae-Leaw, T., Karnjanapratum, S., O’Callaghan, Y. C., O’Keefe, M. B., FitzGerald, R. J., O’Brien, N. M., & Benjakul, S. (2017). Purification and identification of antioxidant peptides from gelatin hydrolysate of seabass skin. *Journal of Food Biochemistry*, 41(3), e12350. <https://doi.org/10.1111/jfbc.2017.41.issue-310.1111/jfbc.12350>.

Saha, S., Buttari, B., Panieri, E., Profumo, E., & Saso, L. (2020). An overview of Nrf2 signaling pathway and its role in inflammation. *Molecules*, 25(22), 5474. <https://doi.org/10.3390/molecules25225474>.

Sheng, J., Yang, X., Chen, J., Peng, T., Yin, X., Liu, W., ... Yang, X. (2019). Antioxidative effects and mechanism study of bioactive peptides from defatted walnut (*Juglans*

- regia L.) meal hydrolysate. *Journal of Agricultural and Food Chemistry*, 67(12), 3305–3312. <https://doi.org/10.1021/acs.jafc.8b05722>.
- Shi, J., Arunasalam, K., Yeung, D., Kakuda, Y., Mittal, G., & Jiang, Y. (2004). Saponins from edible legumes: Chemistry, processing, and health benefits. *Journal of medicinal food*, 7(1), 67–78.
- Soskić, S. S., Dobutović, B. D., Sudar, E. M., Obradović, M. M., Nikolić, D. M., Djordjevic, J. D., ... Isenović, E. R. (2011). Regulation of inducible nitric oxide synthase (iNOS) and its potential role in insulin resistance, diabetes and heart failure. *Open Cardiovascular Medicine Journal*, 5, 153–163. <https://doi.org/10.2174/1874192401105010153>.
- Wang, F., Weng, Z., Lyu, Y.i., Bao, Y., Liu, J., Zhang, Y.u., ... Shen, X. (2020). Wheat germ-derived peptide ADWGGPLPH abolishes high glucose-induced oxidative stress via modulation of the PKC ζ /AMPK/NOX4 pathway. *Food & Function*, 11(8), 6843–6854. <https://doi.org/10.1039/D0FO01229G>.
- Wang, W. Y., Zhao, Y. Q., Zhao, G. X., Chi, C. F., & Wang, B. (2020). Antioxidant peptides from collagen hydrolysate of redlip croaker. *Mar Drugs*, 18(3). <https://doi.org/10.3390/md18030156>.
- Xu, Q., Yan, X., Zhang, Y., & Wu, J. (2019). Current understanding of transport and bioavailability of bioactive peptides derived from dairy proteins: A review. *International Journal of Food Science and Technology*, 54(6), 1930–1941. <https://doi.org/10.1111/ijfs.2019.54.issue-6>.
- Zanoni, C., Aiello, G., Arnoldi, A., & Lammi, C. (2017). Hempseed peptides exert hypocholesterolemic effects with a statin-like mechanism. *Journal of Agricultural and Food Chemistry*, 65(40), 8829–8838. <https://doi.org/10.1021/acs.jafc.7b02742>.
- Zhang, Q., Tong, X., Li, Y., Wang, H., Wang, Z., Qi, B., ... Jiang, L. (2019). Purification and characterization of antioxidant peptides from alcalase-hydrolyzed soybean (*Glycine max* L.) hydrolysate and their cytoprotective effects in human intestinal caco-2 cells. *Journal of Agricultural and Food Chemistry*, 67(20), 5772–5781. <https://doi.org/10.1021/acs.jafc.9b01235>.
- Zhu, W., Ren, L., Zhang, L.i., Qiao, Q., Farooq, M. Z., & Xu, Q. (2020). The potential of food protein-derived bioactive peptides against chronic intestinal inflammation. *Mediators of Inflammation*, 2020, 1–15. <https://doi.org/10.1155/2020/6817156>.